scientific data

OPEN

DATA DESCRIPTOR

Transcriptome and translatome profiling of Col-0 and *grp7grp8* under ABA treatment in *Arabidopsis*

Jing Zhang[1,2,4], Yongxin Xu[1,2,4] & Jun Xiao[1,2,3] ✉

Abscisic acid (ABA) is a crucial phytohormone that regulates plant growth and stress responses. While substantial knowledge exists about transcriptional regulation, the molecular mechanisms underlying ABA-triggered translational regulation remain unclear. Recent advances in deep sequencing of ribosome footprints (Ribo-seq) enable the mapping and quantification of mRNA translation efficiency. Additionally, RNA-binding proteins (RBPs) play essential roles in translational regulation by interacting with target RNA molecules, making the identification of binding sites via UV crosslinking and immunoprecipitation (CLIP) critical for understanding RBP function. Glycine-rich RNA-binding proteins (GRPs), a prominent class of RBPs in plants, are responsive to ABA. In this study, RNA-seq and Ribo-seq analyses were conducted on 3-day-old Col-0 and *grp7grp8* seedlings of *Arabidopsis thaliana*, treated with either ABA or mock solutions. These analyses facilitated deep sequencing of total mRNA and mRNA fragments protected by translating ribosomes. Additionally, CLIP-seq analysis of *pGRP7::GRP7-GFP grp7-1* identified RNA bound by GRP7. This multi-omics dataset allows for a comprehensive investigation of the plant's response to ABA from various perspectives, providing a significant resource for studying ABA-regulated mRNA translation efficiency.

Background & Summary

Abscisic acid (ABA) is a vital phytohormone that regulates plant development and responses to environmental stresses[1]. In the presence of ABA, the ABA receptors PYRABACTIN RESISTANCE1/ PYRABACTIN-LIKE/ REGULATORY COMPONENTS OF ABA RECEPTORS (PYR/PYL/RCAR) form a complex with PROTEIN PHOSPHATASE 2Cs (PP2Cs). This complex inhibits the phosphatase activity of PP2Cs, thereby activating SNF1-RELATED PROTEIN KINASE 2 s (SnRK2s). Activated SnRK2s, in turn, stimulates ABRE-binding protein/ABRE-binding factor (AREB/ABF) transcription factors, leading to the enhanced transcription of ABA-responsive genes[1,2]. In addition to activating downstream transcriptional regulation, findings indicate that ABA also inhibits global protein translation[3,4]. However, the specific changes in mRNA translation efficiency regulated by ABA signaling, along with the underlying regulatory mechanisms, remain poorly understood. Thus, further investigation into the complex interplay between ABA signaling and translational regulation is crucial for a deeper understanding of how ABA governs plant responses to environmental cues.

Protein expression undergoes greater evolutionary constraints than mRNA levels, with translation efficiency playing a pivotal role in shaping protein levels during cellular adaptation to various stimuli[5,6]. Given the challenge of accurately monitoring translation compared to measuring mRNA levels, historical efforts in globally monitoring gene expression have primarily concentrated on measuring mRNA levels. However, translational control is an essential and regulated step in determining levels of protein expression[6,7]. This has changed with the development of Ribo-seq, a deep-sequencing-based tool enabling detailed measurement of translation globally and *in vivo*, was developed and first described in 2009[8]. The sequencing of these ribosome-protected fragments is termed ribosome footprints[9]. This approach provides comprehensive insights into changes in mRNA translation efficiency, enabling researchers to explore the intricacies of post-transcriptional regulation and its influence on cellular protein expression. By quantifying the density of protected fragments on a specific transcript,

[1]Key Laboratory of Plant Cell and Chromosome Engineering, Institute of Genetics and Developmental Biology, Chinese Academy of Sciences, Beijing, 100101, China. [2]University of Chinese Academy of Sciences, Beijing, 100049, China. [3]CAS-JIC Centre of Excellence for Plant and Microbial Science (CEPAMS), Institute of Genetics and Developmental Biology, CAS, Beijing, 100101, China. [4]These authors contributed equally: Jing Zhang, Yongxin Xu. ✉e-mail: jxiao@genetics.ac.cn

researchers can estimate the rate of protein synthesis. Furthermore, identifying the locations of these protected fragments facilitates the empirical determination of the translated products, revealing new open reading frames (ORFs) and potentially prompting revisions in the annotation of known genes. Additionally, the pattern of ribosome footprints can be utilized to identify regulatory translation pauses and translated upstream open reading frames (uORFs)[9–11]. Understanding translation dynamics is essential for comprehending post-transcriptional regulation closely linked to cellular protein levels.

The regulation of translation involves a diverse spectrum of RNA-binding proteins (RBPs) that play significant roles in the complex process of protein synthesis[12,13]. Among the RBPs, glycine-rich RNA binding proteins (GRPs) are associated with abiotic stresses[14]. Notably, GRP7, which contains an N-terminal RNA recognition motif and a C-terminal glycine-rich domain, is linked to various biotic and abiotic stresses, including ABA treatment, temperature fluctuations, drought, and salinity[14–16]. GRP7 exerts multiple functions in RNA processing, such as alternative splicing of precursor mRNA, primary microRNA processing, and acting as a shuttle protein that facilitates mRNA export from the nucleus to the cytoplasm under cold stress[15–18]. Furthermore, GRP7 plays a crucial role in translation regulation. Elevated temperatures rapidly induce GRP7 condensates, and its liquid–liquid phase separation (LLPS) in the cytoplasm contributes to the formation of stress granules that sequester RNA and inhibit translation[19]. Additionally, GRP7 is implicated in innate immunity and interacts with various components of the translational machinery, including eukaryotic translation initiation factor (eIF4A1, eIF4A2, eIF4E), and ribosomal protein uS11z (uS11z)[20]. GRP8, another member of the GRP family, exhibits high sequence similarity to GRP7 and functional redundancy with it[4,21]. Double mutants for GRP7 and GRP8 display hypersensitivity to ABA during cotyledon greening, and GRP7 protein level decrease sharply upon ABA treatment[4]. However, whether and how GRP7 and GRP8 are involved in ABA-mediated translation regulation remains unclear.

In this study, we present RNA-seq and Ribo-seq data of 3-day-old seedlings of Col-0 and *grp7grp8*, treated with either 5 μM ABA or mock solution. These assays enabled us to generate a genome-wide transcriptome and translatome for association analysis. Additionally, we utilized CLIP-seq to identify the RNA targets of GRP7 under both ABA treatment and control conditions during early seedling development. Our findings provide a valuable dataset from Ribo-seq and CLIP-seq analyses, establishing a novel molecular link between ABA signaling and the regulation of translation, elucidating the interplay between GRP7 and ABA-mediated translational regulation.

Methods

Sample collection. *Arabidopsis thaliana* seeds of wild type Col-0, *grp7grp8* double mutants[4] and *pGRP7::GRP7-GFP grp7-1* complementary line[22] were first sterilized with 75% ethanol supplemented with 0.1% Triton X-100. Subsequently, the seeds were sown onto plates containing half-strength Murashige and Skoog (MS) medium, adjusted to pH 5.7, and supplemented with 1% (w/v) sucrose and 0.8% (w/v) agar. The plates were then subjected to vernalization in the dark at 4 °C for three days, followed by growth under long-day conditions (16 hours of light/8 hours of darkness) at 22 °C for an additional three days in a light incubator. Thereafter, 3-day-old seedlings were transferred to filter paper moistened with 1/2 MS liquid medium containing 5 μM ABA or an equivalent volume of mock solution, and incubated under the same long-day conditions at 22 °C for 4 hours. The seedlings were then gently dried and flash-frozen in liquid nitrogen. The samples were stored at −80 °C for further analysis.

RNA sequencing (RNA-seq). Three-day-old seedlings of the Col-0 and *grp7grp8* genotypes, treated with either 5 μM ABA or a mock solution, were harvested for RNA sequencing. RNA was isolated from these samples using the Quick RNA Isolation Kit (Huayueyang) according to the manufacturer's protocol. The extracted RNA samples were then sequenced on the Illumina NovaSeq6000 platform to generate transcriptomic data.

Data processing of RNA-seq data. Raw reads of RNA-seq were firstly filtered by fastp (v0.20.1)[23] with parameter "--detect_adapter_for_pe" for adapters removing, low-quality bases trimming, and reads filtering. The obtained clean reads were subsequently aligned to the *Arabidopsis thaliana* reference genome (TAIR10) using STAR (v2.7.10)[24] with default parameters. Quantification of reads that mapped to each gene was counted using featureCounts (v2.0.1)[25] with the parameter "-p -P -B -C" for RNA-seq. The raw counts of RNA-seq were used as inputs for differentially expression analysis by DESeq2 (v1.26.0)[26] and further normalized to FPKM (Fragments per kilobase per million mapped reads). FPKM values of gene expression were Z-scaled and clustered by k-means method and displayed using R package ComplexHeatmap (v2.4.3)[27].

Deep sequencing of ribosome footprints (Ribo-seq). The overview of the library construction of Ribo-Seq[28,29] is illustrated in Fig. 1a.

Sample lysis. The 3-day-old seedlings (0.2 g) of Col-0 and *grp7grp8* with 5 μM ABA or mock were grounded in liquid nitrogen followed by resuspension in 600 μL ice-cold lysis buffer that was composed of 20 mM Tris-HCl (pH 7.4), 150 mM NaCl, 5 mM $MgCl_2$, 1% Triton X-100, with 1 mM DTT, 100 ug/mL cycloheximide (CHX) and 25 U/mL Turbo DNase added freshly. Clarifying the lysate by centrifugation for 10 min at 20,000 *g* under 4 °C, the soluble supernatant was recovered.

Partial RNA digestion. 6 μL of RNase I (100 U/μL) was added to 600 μL lysate and incubated for 45 min at room temperature with gentle mixing. Digestion was stopped by the addition of 10 μL SUPERase-In RNase inhibitor (Invitrogen Cat# AM2694).

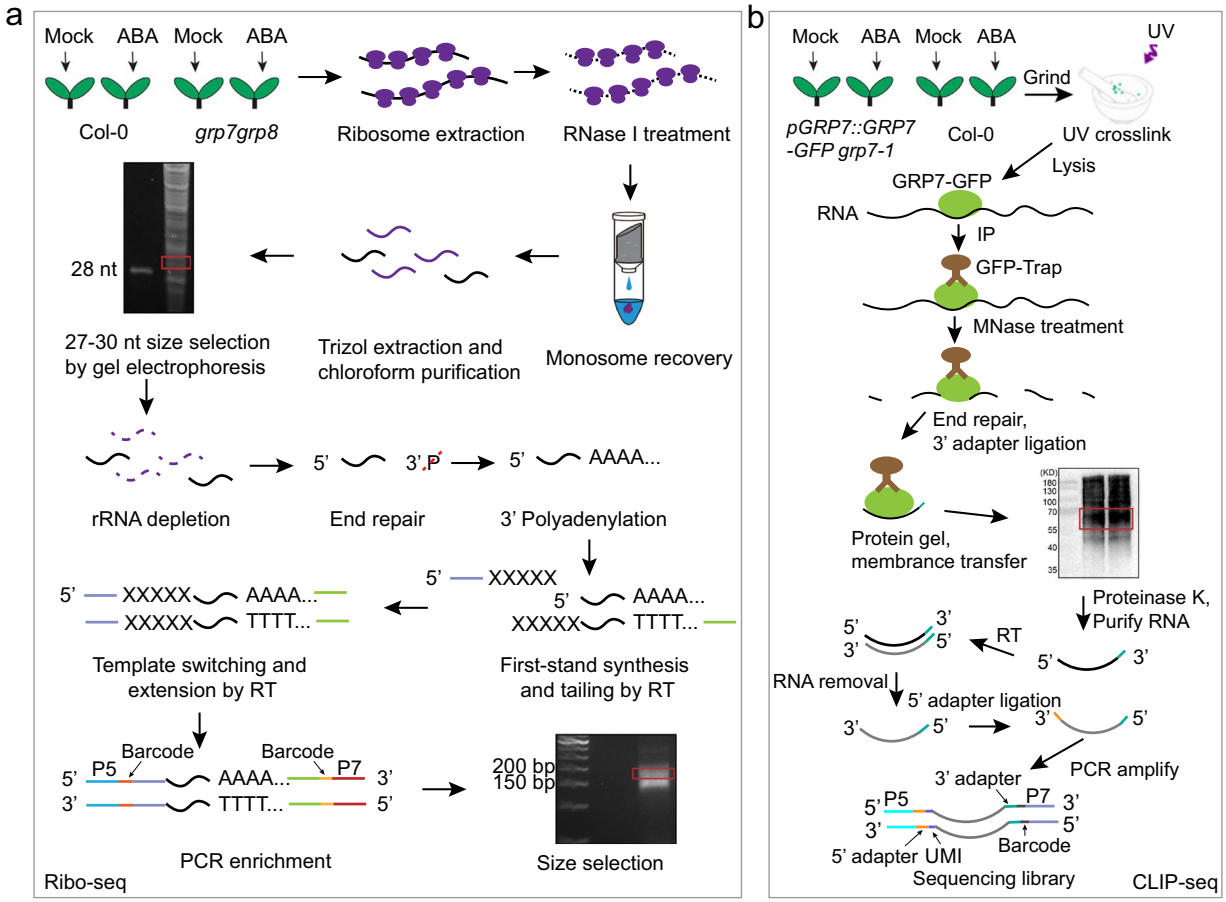

Fig. 1 Experimental design and workflow of Ribo-seq and CLIP-seq. (**a**) The sequencing library construction protocol for Ribo-seq. (**b**) The sequencing library construction protocol for CLIP-seq. P5 and P7 were PCR primer, Unique Molecular Identifier (UMI) was random sequence.

Isolation of ribosome-protected RNA fragments. Meanwhile, MicroSpin S-400 HR columns (GE Healthcare Cat# 275140-01) were equilibrated with 3 mL of polysome buffer, which was composed of 20 mM Tris-HCl (pH 7.4), 150 mM NaCl, 5 mM $MgCl_2$, with 1 mM DTT and 100 ug/mL CHX added freshly, by gravity flow and emptied by centrifugation at 600 *g* for 4 min. Then digested lysate was immediately loaded on the column and eluted from the column by centrifugation at 600 *g* for 2 min at 4 °C.

RNA extraction and size selection. The RNA was extracted from the flow-through using Trizol (Thermo Fisher, 15596018CN) and further purified by chloroform and isopropanol precipitation. The RNA was separated by electrophoresis for 65 min at 200 V using 15% denaturing urea-PAGE gel. The ribosome-protected RNA fragments (RPF) of between 27 nt to 30 nt was cut and eluted in 800 μL of RNA gel extraction buffer, which was composed of 300 mM sodium acetate pH 5.2, 1 mM EDTA, and 0.25% (w/v) SDS, overnight at room temperature with gentle mixing. Precipitate RNA by 800 μL isopropanol and 1 μL GlycoBlue with mixing. Resuspend size-selected RNA in 10 μL DEPC H_2O and transfer to a clean RNase-free microfuge tube.

Remove of rRNA. The rRNA fragments were removed using the Ribo-off rRNA depletion kit (Plant) (Vazyme, N409). Purify RNA using the Zymo column cleanup-RNA Clean & Concentrator-5 columns (Cat R1016) according to the manufacturer's instructions.

3′ end dephosphorylation. The mRNAs were dephosphorylated by PNK mix (60 μL 5X PNK pH 6.5 buffer, 3 μL 0.1 M DTT, 5 μL RNase Inhibitor, 7 μL T4 PNK, add DEPC H_2O to 300 μL) and incubated for 20 min at 37 °C with 1000 rpm shaking. Purify RNA using the Zymo column cleanup-RNA Clean & Concentrator-5 columns.

Library preparation. The RNA fragments were subjected into library generation using Smarter smRNA-Seq kit (Takara Cat# 635031) according to the manufacturer's instructions. The final library of approximately 180 bp was size-selected by gel electrophoresis for 90 min at 100 V using a 3% agarose gel. The constructed library was sequenced on the Illumina NovaSeq6000 platform.

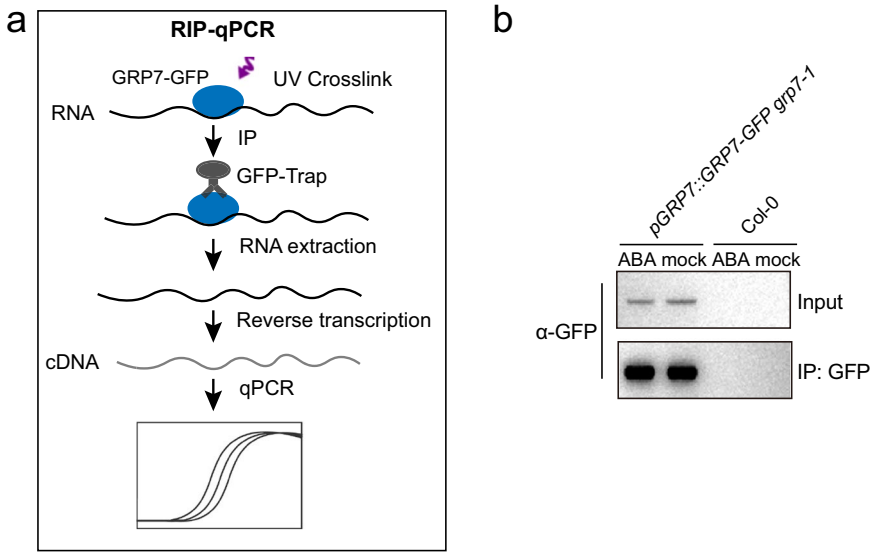

Fig. 2 Workflow and quality control of RIP-qPCR. (**a**) The workflow of RIP-qPCR. (**b**) Western blot analysis was utilized to assess the immunoprecipitation efficiency of GRP7-GFP in RIP experiments.

Ribo-seq data processing. For Ribo-seq data analysis, we exclusively utilized the first sequencing reads (*_R1.fq.gz) and filtered by fastp (v0.20.1)[23] with parameter "-a AAAAAAAAAA -f 3 -l 16". The filtered reads were firstly aligned against the non-coding RNA sequences of *A. thaliana* downloaded from Ensembl Plants[30] using bowtie2[31] to produce the unaligned reads. Subsequently, these unaligned reads were mapped to reference genome using STAR (v2.7.10)[24] with parameters "--outFilterMismatchNmax 2 --outFilterMultimapNmax 1 --outFilterMatchNmin 14 --alignEndsType EndToEnd". The number of reads that mapped to each gene was counted using featureCounts (v2.0.1)[25] with default parameters. The processed raw counts were further normalized to RPKM (Reads per kilobase per million mapped reads) values and used as inputs for differentially expression analysis by DESeq2 (v1.26.0)[26].

Analysis of translational efficiency. Genes with expression levels exceeding 1 RPKM in Ribo-seq and 1 FPKM in RNA-seq were kept for the calculation of translation efficiency (TrE). TrE was determined by comparing the transcription and translation rates of genes, calculated as the ratio of average RPKM values from Ribo-seq to FPKM values from RNA-seq. The formula is $RPKM_{Ribo\text{-}seq}/FPKM_{RNA\text{-}seq}$. To further explore the dynamics of translation, we utilized the Xtail package (v1.1.5)[32] for calculating differential translation efficiencies across the dataset. The raw counts matrix obtained from RNA-seq and Ribo-seq were utilized as input for Xtail, with a significant threshold set at an adjusted p-value < 0.05 to determine differential translational efficiency.

Crosslinking and immunoprecipitation and high-throughput sequencing (CLIP-seq). The overview of the library construction of CLIP-Seq[33,34] is illustrated in Fig. 1b.

UV-crosslinking. The 3-day-old seedlings (1 g) of Col-0 and *pGRP7::GRP7-GFP grp7-1*, treated with either 5 μM ABA or mock solution, were ground to powder using liquid nitrogen and then crosslinked twice at 600 mJ/cm^2 in a UVP crosslinker (Analytik jena).

Immunoprecipitation. The powder was lysed by 1.5 mL ice-cold iCLIP lysis buffer that was composed of 50 mM Tris-HCl (pH 7.4), 100 mM NaCl, 1% IGEPAL®CA-630, 0.1% SDS, 0.5% sodium deoxycholate and protease inhibitor added freshly. Clarifying the lysate by centrifugation for 15 min at 12000 rpm under 4 °C, the soluble supernatant was recovered. 45 μL of DNase I (NEB, M0303L) was added to 1.5 mL lysate and incubated for 5 min at 37 °C with 1000 rpm shaking. Place the lysate on ice for 5 minutes, then clarify it by centrifugation at 12000 rpm for 15 minutes at 4 °C. After centrifugation, recover the soluble supernatant. The RNA-protein complexes (RNP) were enriched from the lysate by immunoprecipitation using GFP-Trap beads (Lablead, GNM-25-1000) for 2 h at 4 °C with constant rotation. Collect the beads on the magnetic stand, discard the supernatant and wash the beads 2x with 1 mL cold Wash buffer (1x PBS, 0.1% SDS, 0.5% deoxycholate, 0.5% IGEPAL®CA-630), 2x with 1 mL cold High salt wash buffer (5x PBS, 0.1% SDS, 0.5% deoxycholate, 0.5% IGEPAL®CA-630) and 2x with 1 mL cold PNK buffer (50 mM Tris-HCl pH 7.4, 10 mM $MgCl_2$, 0.5% IGEPAL®CA-630).

Partial RNA digestion. RNAs on beads were partially digested by micrococcal nuclease (2×10^{-5} U/μL, Takara, 2910 A) incubated for 10 min at 37 °C with 1000 rpm shaking. Wash the beads 2x with 1 mL cold PNK + EGTA buffer (50 mM Tris-HCl pH 7.4, 20 mM EGTA, 0.5% IGEPAL®CA-630), 2x with 1 mL cold Wash buffer and 2x with 1 mL cold PNK buffer.

Name	Forward primer sequence (5′-3′)	Reverse primer sequence (5′-3′)
GRP7	GCGACGTTATTGATTCCAAG	CGCATCCTTCATGGCTTT
HSPRO2	GCGATGAAGCTTTACGCGAG	GTTCATCTCCGCACTTCCCA
CCL	GCTGAAGCATGCGAAGTAATC	CTGTCAACGGGCTCTGAAG
ASPG1	TTTCTTTCTCTCCTCGCCGT	TGGTGAGTGAGGAACGAGTC
SVB2	GTTCAAGACACCGACCACAC	CAGCCTCCTTGATTGCAACA
RHIP1	ATTGGTGTCGCTGCTAGTCT	TAAAGCCGTCCTCTCAAGCA

Table 1. Primers used in RIP-qPCR assay.

Gene type	Condition	Replicate	Number of raw reads	Number of clean reads	Number of mapped reads	Percentage of mapped reads (%)
Col-0	Mock	1	11,853,539	11,657,671	11,288,456	96.83
		2	11,970,758	11,728,287	11,346,928	96.75
		3	11,483,643	11,280,723	10,854,437	96.22
	ABA	1	11,270,781	11,117,391	10,292,940	92.58
		2	11,423,784	11,261,007	10,671,491	94.76
		3	11,463,794	11,326,890	10,539,262	93.05
grp7grp8	Mock	1	11,376,537	11,206,438	10,332,340	92.20
		2	12,224,333	12,023,968	11,618,924	96.63
		3	11,394,860	11,215,903	10,897,650	97.16
	ABA	1	11,530,883	11,302,005	10,936,857	96.77
		2	11,371,427	11,141,485	10,784,762	96.80
		3	11,454,954	11,217,286	10,465,179	93.30

Table 2. Summary of the RNA-seq reads.

3′ end dephosphorylation and 3′ linker ligate RNA. The RNAs on beads were dephosphorylated by PNK mix (60 μL 5X PNK pH 6.5 buffer, 3 μL 0.1 M DTT, 5 μL RNase Inhibitor, 7 μL T4 PNK, 225 μL DEPC H_2O) and incubated for 20 min at 37 °C with 1000 rpm shaking. Wash the beads 2x with 1 mL cold Wash buffer, 2x with 1 mL cold High salt wash buffer and 2x with 1 mL cold 1X Ligase buffer (50 mM Tris-HCl pH 7.5, 10 mM $MgCl_2$). RNAs on beads were ligated 3' RNA linker by 3' ligation mix (3 μL 10X Ligase buffer, 0.3 μL 0.1 M ATP, 0.8 μL 100% DMSO, 9 μL 50% PEG8000, 0.4 μL RNase Inhibitor, 2.5 μL RNA Ligase high conc, 2.5 μL RNA adapters, 11.5 μL DEPC H_2O) and flick to mix, and incubate for 75 min at room temperature. Wash the beads 2x with 1 mL cold Wash buffer, 2x with 1 mL cold High salt wash buffer and 2x with 1 mL cold PNK buffer. Elute into 5 μL 5X SDS loading buffer and 20 μL DEPC H_2O for 10 min at 70 °C with 1200 rpm shaking.

SDS-PAGE and nitrocellulose transfer. Load 20 μL of the eluate onto a 4-12% NuPAGE BisTris polyacrylamide gel for electrophoresis. For better excision leave out at least one well between the two sample. Run for using MOPS SDS running buffer and subsequently blot onto nitrocellulose for 2 hours at 200 mA on ice. Cut lane from nitrocellulose from the RBP band to 20 kDa above it. Cut the membrane area into pieces and transfer them to a fresh 2 mL tube.

Proteinase K digestion and cleanup RNA. Add 200 μL Proteinase K mix (160 μL PK buffer and 40 μL Proteinase K), Digest for 20 min at 37 °C with 1200 rpm shaking. Add 200 μL fresh Urea/PK buffer (420 mg Urea in PK buffer to final volume of 1 mL) and incubate for 20 min at 37 °C with 1200 rpm shaking. Add 400 μL acid phenol: chloroform: isoamyl alcohol (25:24:1, v/v) and mix well, incubate for 5 min at 37 °C with 1200 rpm shaking. Spin briefly, transfer all except membrane slices to a fresh 2 mL tube, incubate for 5 min at 37 °C with 1200 rpm shaking. Centrifuge at 13000 *g*, 15 min, room temperature. Transfer 400 μL aqueous layer to new 15 mL tube. Purify RNA using the Zymo column cleanup-RNA Clean & Concentrator-5 columns (Cat R1016) according to the manufacturer's instructions.

Reverse transcription. Mix 10 μL of RNA with 0.5 μL AR17 primer, heat at 65 °C for 2 min in a pre-heated PCR block, place immediately on ice. Add 10 μL reverse transcription mix (2 μL 10x AffinityScript Buffer, 2 μL 0.1 M DTT, 0.8 μL 25 mM dNTPs, 0.3 μL RNase Inhibitor, 0.9 μL AffinityScript Enzyme, 4 μL DEPC H_2O) to each sample, mix well, incubate 55 °C, 45 min in a pre-heated PCR block.

Cleanup cDNA. Add 3.5 μL ExoSAP-IT to each sample and mix well, incubate for 15 min at 37 °C. Add 1 μL 0.5 M EDTA and mix well, and add 3 μL 1 M NaOH and mix well, incubate for 12 min at 70 °C, and add 3 μL 1 M HCl and mix well. MyONE Silane beads cleanup cDNA (Prepare beads: Magnetically separate 10 μL MyONE Silane beads per sample, remove supernatant; Wash 1x with 500 μL RLT buffer; Resuspend beads in 93 μL RLT buffer.

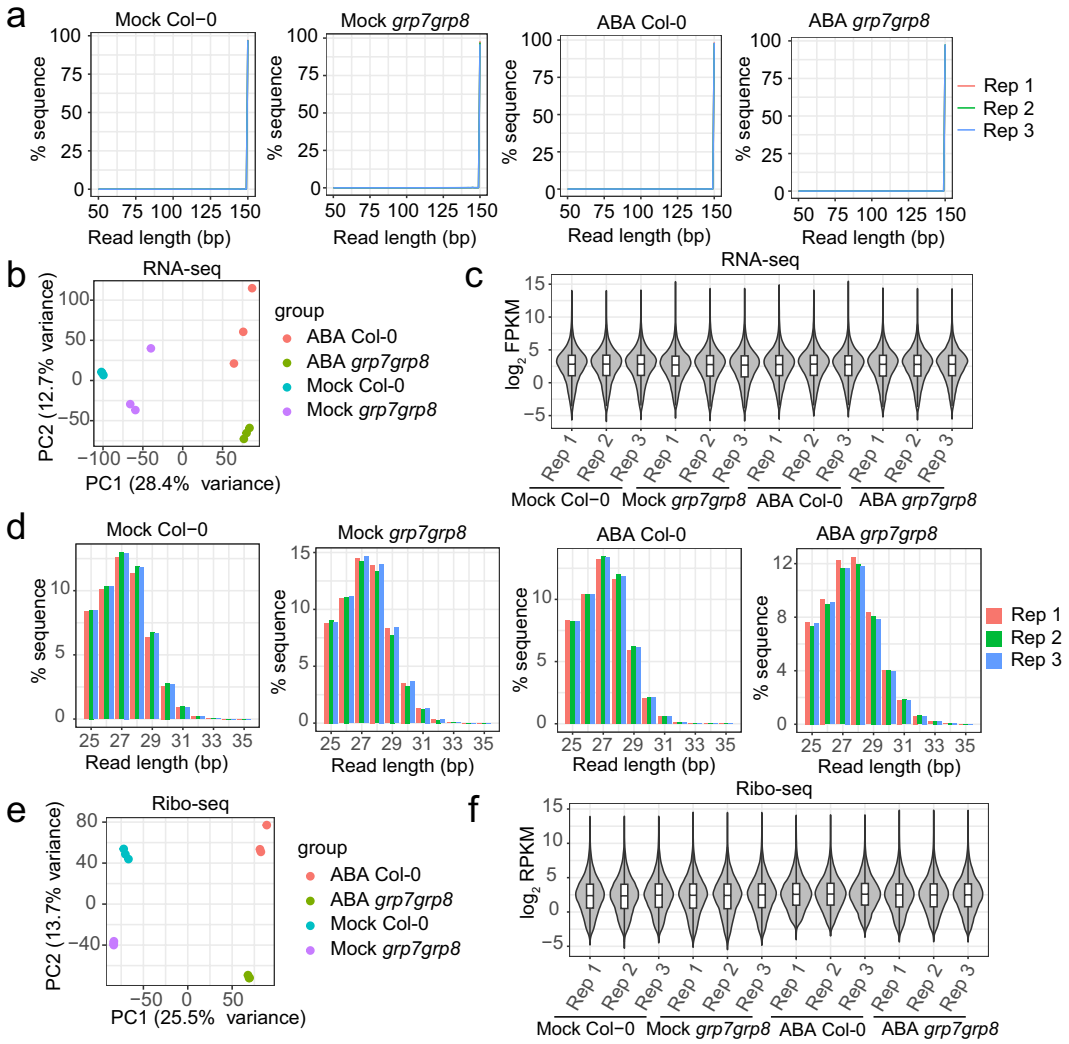

Fig. 3 Reads quality and technical validation of RNA-seq and Ribo-seq samples of Col-0 and *grp7grp8* with ABA or mock treatment. (**a**) Length distribution of clean reads from RNA-seq. (**b**) PCA plot of RNA-seq mapped reads of each gene. (**c**) Violin and box plot of the $\log_2$ FPKM of RNA-seq. (**d**) Length distribution of clean reads from Ribo-seq. (**e**) PCA plot of Ribo-seq mapped reads of each gene. (**f**) Violin and box plot of the $\log_2$ RPKM of Ribo-seq.

Bind RNA: Add beads in 93 μL RLT buffer to sample, mix; Add 111.6 μL 100% EtOH; Pipette mix, leave pipette tip in tube, pipette mix twice, for 5 min. Magnetically separate, remove supernatant; Add 1 mL 80% EtOH, pipette resuspend and move to new tube; After 30 s, magnetically separate, remove supernatant; Wash 2x with 80% EtOH; Spin briefly, magnetically separate, remove residual liquid with fine tip; Air-dry 5 min. Resuspend in 5 μL 5 mM Tris-HCl pH 7.5. Let sit for 5 min, do not remove from beads.)

5′ linker ligate cDNA. On MyONE Silane beads, add 0.8 μL 5′ adapter and 1 μL 100% DMSO to 5 μL cDNA on beads, heat at 75 °C, 2 min, place immediately on ice. Add 12.8 μL ligation mix (2 μL 10x NEB RNA Ligase Buffer, 0.2 μL 0.1 M ATP, 9 μL 50% PEG8000, 0.5 μL RNA Ligase high conc, 1.1 μL H_2O) to each sample, mix sample with pipette tip. Add another 1 μL RNA Ligase high conc to each sample, flick to mix, and incubate at room temperature overnight. MyONE Silane beads cleanup linker-ligated cDNA.

PCR amplify cDNA. Prepare PCR master mix (25 μL 2X seqAmp PCR Buffer, 12 μL Nuclease-Free H_2O, 1 μL seqAmp DNA Polymerase) for all reactions, add 38 μL PCR master mix to each sample (10 μL), then add 1 μL of each Forward and Reverse primer, mix well. Run the plate with the following program in the PCR machine: 98°C 1 min, 5 cycles of: 98°C 10 s, 60°C 5 s, 68°C 10 s. qPCR quantitation: The 5 μL PCR sample was taken from the tube and prepared into a 15 μL qPCR mix. The final number of PCR cycles was determined according to the ct value of qPCR. Continue to run the plate in the PCR machine to final number of PCR cycles.

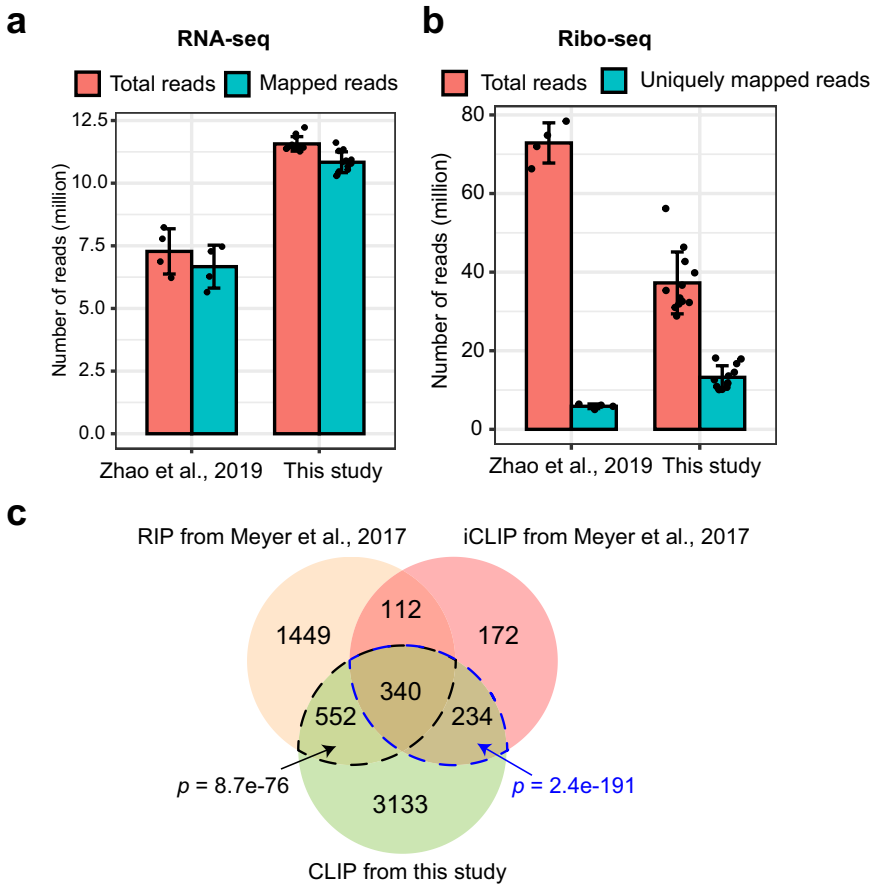

Fig. 4 Statistics of sequencing data and results in this study and published data. (**a**) Number of total reads and mapped reads in RNA-seq libraries of Zhao *et al.*[34] and this study. The statistic data is derived from Table S10 in Zhao *et al.*[34]. (**b**) Number of total reads and uniquely mapped reads in Ribo-seq libraries of Zhao *et al.*[34] and this study. The statistic data is derived from Table S9 in Zhao *et al.*[34]. (**c**) Venn diagrams of GRP7 target genes identified through different methods. RIP-seq and iCLIP-seq results are derived from Table S2 and S4 in Meyer *et al.*[22], respectively, while the CLIP-seq results are obtained from this study. Hypergeometric tests were used to calculate the *p* values for the enrichment of genes.

Cleanup library. The final library of approximately 150-200 bp was size-selected by gel electrophoresis for 90 min at 100 V using a 3% agarose gel. The constructed library was sequenced on the Illumina NovaSeq6000 platform.

CLIP-seq data processing. The initial processing of CLIP-seq was conducted using fastp (v0.20.1)[23] with parameter "--adapter_sequence TGGAATTCTCGG --adapter_sequence_r2 GATCGTCGGACT" set for filtering raw reads. Then the resulting clean reads were aligned to the reference genome using STAR (v2.7.10)[24] with no more than two mismatches, ensuring high accuracy in reads mapping[24]. To enhance the quality and reliability of the results, Picard (v2.23.3) was employed to remove duplicates among the mapped reads, thereby reducing potential bias introduced by PCR amplification or sequencing artifacts.

GRP7 binding site identification. The GRP7 binding sites were identified by performing CLIP-seq peak calling using CLIPper (v0.1.4)[35] with default parameters. Then, bedtools[36] was used to retain the peaks consistently observed across two biological replicates, ensuring robustness of results. Significant GRP7 binding sites were defined as those exclusively present in IP samples yet absent in negative controls. The identified GRP7 binding peaks were annotated against the *Arabidopsis thaliana* genome using the "annotatePeak" function in R package ChIPseeker (v1.26.2)[37]. Gene promoters were defined as regions 1.5 Kb upstream from the transcription start site (TSS). The GRP7-binding efficiency of a gene was determined by calculating the ratio of CLIP-seq CPM values (Counts per million) to mRNA-seq FPKM values.

RNA-immunoprecipitation-qPCR (RIP-qPCR). The overview of the workflow of RIP-qPCR[38] is illustrated in Fig. 2a. One gram of 3-day-old Col-0 and *pGRP7::GRP7-GFP grp7-1* were treated with 5 μM ABA or mock for 4 hours and were UV-treat twice, each with the irradiation intensity at 600 mJ/cm^2. The plant was ground to powder with liquid nitrogen, and solubilized with 2 mL of extraction buffer (50 mM Tris-HCl pH 8.0,

Type	Samples	Samples group	Pearson correlation coefficient
RNA-seq	Mock Col-0	rep1 vs. rep2	0.992
		rep1 vs. rep3	0.991
		rep2 vs. rep3	0.991
	Mock *grp7grp8*	rep1 vs. rep2	0.988
		rep1 vs. rep3	0.987
		rep2 vs. rep3	0.991
	ABA Col-0	rep1 vs. rep2	0.986
		rep1 vs. rep3	0.987
		rep2 vs. rep3	0.99
	ABA *grp7grp8*	rep1 vs. rep2	0.992
		rep1 vs. rep3	0.99
		rep2 vs. rep3	0.989
Ribo-seq	Mock Col-0	rep1 vs. rep2	0.984
		rep1 vs. rep3	0.983
		rep2 vs. rep3	0.983
	Mock *grp7grp8*	rep1 vs. rep2	0.989
		rep1 vs. rep3	0.987
		rep2 vs. rep3	0.987
	ABA Col-0	rep1 vs. rep2	0.966
		rep1 vs. rep3	0.967
		rep2 vs. rep3	0.97
	ABA *grp7grp8*	rep1 vs. rep2	0.983
		rep1 vs. rep3	0.983
		rep2 vs. rep3	0.982
CLIP-seq	Mock *pGRP7::GRP7-GFP grp7*	rep1 vs. rep2	0.847
	ABA *pGRP7::GRP7-GFP grp7*	rep1 vs. rep2	0.887

Table 3. Pearson correlation coefficient between different biological replicates of RNA-seq, Ribo-seq and CLIP-seq samples.

150 mM NaCl, 4 mM $MgCl_2$, 0.1% Igepal CA-630, 5 mM DTT, 0.1% SDS, 1 mM PMSF, protease inhibitor, and 80 U/mL SUPERase-In RNase inhibitor). 100 μL supernatant was used as input. The RNA-GRP7-GFP complexes were enriched from the remaining supernatant by immunoprecipitation using GFP-trap beads for 2 h at 4 °C with constant rotation. The GFP-Trap beads were washed with washing buffer (50 mM Tris-HCl pH 8.0, 150 mM NaCl, 2 mM EDTA, 1% Igepal CA-630, and 0.1% SDS) four times. To elute the protein–RNA complexes, the beads were incubated with 50 μL of RIP elution buffer (100 mM Tris-HCl pH 7.4, 100 mM NaCl, 10 mM EDTA, 1% SDS and 80 U/mL RNase inhibitor) at room temperature for 10 min with rotation. The protein was degraded by proteinase K, and co-precipitated RNAs were eluted by 1 mL TRIzol of RNA extraction reagent. The RNA sample was incubated with DNase I and reverse-transcribed using cDNA synthesis kit (TIANGEN, KR116) for qPCR. In parallel, input samples were used for quantification. The primers used for qPCR are listed in Table 1.

Data Records

The raw sequence data of RNA-seq, Ribo-seq, and CLIP-seq in this study were deposited in the Genome Sequence Archive (https://bigd.big.ac.cn/gsa)[39] in National Genomics Data Center[40] under accession number CRA012798[41] and also been deposited in the National Center for Biotechnology Information (NCBI) Sequence Read Archive under BioProject accession number PRJNA1157223[42].

Technical Validation

RNA-seq reads quality validation. A total of 12 RNA-Seq runs were conducted, with each sample yielding at least 11 million reads. After trimming the sequencing reads based on quality scores and nucleotide length, over 97.9% of the reads were retained, with almost all clean reads measuring 150 bp (Table 2, Fig. 3a), consistent with the sequencing protocol. This indicates high sequencing quality. The remaining reads were then used as input to generate sequencing quality control (QC) reports using FastQC to validate the quality of the reads.

Assessment of RNA-seq data. All clean reads were mapped to the TAIR10 reference genome, with each library yielding over 10 million mapped reads and achieving a mapping rate exceeding 92% (Table 2). This substantial dataset facilitates accurate gene expression analysis and surpasses the data volume of comparable published study[34] (Fig. 4a). The number of mapped reads for each gene was counted using featureCounts and normalized to FPKM values. Each Col-0 or *grp7grp8* sample included three biological replicates, with Pearson correlation coefficients among these replicates exceeding 0.98 (Table 3). The level of correlation is comparable to or higher than that reported in similar studies[34,43,44], indicating robust reproducibility of our RNA-seq data. Principal component analysis (PCA) was conducted in R using these normalized expression values, confirming

Gene type	Condition	Replicate	Number of raw reads	Number of clean reads	After remove ncRNA	Uniquely mapped reads	Percentage of Uniquely mapped reads (%)	Mapped reads within CDS
Col-0	Mock	1	36,680,665	23,713,458	23,088,433	12,605,586	54.60	3,639,375
		2	31,013,398	21,307,130	20,739,296	11,692,363	56.38	3,223,834
		3	28,838,006	19,599,188	19,090,235	10,712,091	56.11	2,941,111
	ABA	1	32,559,042	23,563,852	23,045,378	13,583,164	58.94	1,293,694
		2	39,828,919	28,784,444	28,110,183	16,714,091	59.46	1,579,503
		3	42,711,145	30,857,713	30,117,546	17,905,645	59.45	1,684,943
grp7grp8	Mock	1	46,342,962	30,062,441	29,115,084	14,516,651	49.86	5,302,471
		2	56,190,279	36,740,995	35,665,597	18,137,651	50.85	6,280,516
		3	35,340,688	23,791,037	23,070,432	11,767,806	51.01	4,062,081
	ABA	1	33,426,634	23,182,728	21,811,662	10,905,432	50.00	2,861,028
		2	32,271,972	22,017,031	20,675,021	10,167,630	49.18	2,694,184
		3	31,895,956	22,071,314	20,701,214	10,096,134	48.77	2,864,056

Table 4. Summary of the Ribo-seq reads.

Gene type	Condition	Replicate	Number of raw reads	Number of clean reads	Number of mapped reads	Percentage of mapped reads (%)
pGRP7::GRP7-GFP grp7-1	Mock	1	28,649,269	22,609,323	5,981,799	26.46
		2	32,064,065	27,653,738	7,460,803	26.98
	ABA	1	26,400,749	22,247,502	5,917,161	26.60
		2	24,888,071	20,469,515	5,277,851	25.78
Col-0	Mock	1	21,904,509	6,940,377	1,371,640	19.76
		2	26,094,680	5,111,750	1,000,950	19.58
	ABA	1	26,725,733	12,828,783	1,868,005	14.56
		2	22,517,618	13,068,141	2,044,487	15.64

Table 5. Summary of the CLIP-seq reads.

the high reproducibility of the sequencing data and clearly distinguishing between different genotypes and treatments (Fig. 3b). The distribution of $\log_2$(FPKM) values ranged broadly from -5 to 15 across different samples (Fig. 3c).

Ribo-seq reads quality validation. In line with the transcriptome analysis, a total of 12 ribosome profiling libraries were constructed, with each library yielding an average of 37.26 million reads (Table 4). The raw sequencing data were initially filtered using fastp, which included trimming poly(A) adapters and filtering out low-quality and short reads. The first three nucleotides of Read 1, originating from the template-switching oligo, were also trimmed before mapping. The processed reads from each sample were then mapped to the non-coding RNA sequence in the TAIR10 genome, and any reads that aligned were removed. During this step, approximately 2.20% to 6.21% of the clean reads were filtered out (Table 4). The majority of the remaining clean reads (unaligned reads) fell within the 25–35 nt range, with 27 or 28 nt representing the largest proportion (Fig. 3d).

Assessment of Ribo-seq data. The remaining clean reads were aligned to the reference genome, with a significant fraction mapping to multiple genomic positions due to highly repetitive regions. Specifically, approximately 6.16 to 13.54 million reads (26.16% to 42.07% of the remaining clean reads) were mapped to multiple loci in the *Arabidopsis thaliana* genome, while 10.10 to 18.14 million reads (48.77% to 59.46% of the remaining clean reads) were uniquely mapped (Table 4). These results indicate that non-specific mapping accounted for a substantial portion of the total mapping reads in the Ribo-seq library. Each Ribo-seq library yielded over 10 million uniquely mapped reads. Notably, despite having fewer raw reads than published studies[34], our libraries demonstrated a higher number of uniquely mapped reads, highlighting their quality (Fig. 4b). For each Ribo-seq sample, three biological replicates were established, with Pearson correlation coefficients exceeding 0.96 among the replicates. This level of correlation is comparable to or higher than that reported in similar studies[34,43,44] (Table 3), indicating strong reproducibility of our Ribo-seq data. PCA confirmed high reproducibility among biological replicates and successfully distinguished between different genotypes and treatments (Fig. 3e). The distribution of $\log_2$(RPKM) values ranged broadly from -5 to 15 across the samples (Fig. 3f).

CLIP-seq reads quality validation. A total of 8 CLIP-Seq libraries were constructed, each yielding approximately 21 to 32 million raw reads. After quality control using fastp, we obtained over 20 million reads for each immunoprecipitated (IP) sample (*pGRP7::GRP7-GFP grp7-1*) and between 5 and 13 million reads for each control sample (Col-0) (Table 5). The length of the clean reads ranges from 15 bp to 150 bp, with the majority falling between 20 bp and 80 bp (Fig. 5a). The remaining reads were analyzed using FastQC to assess read quality.

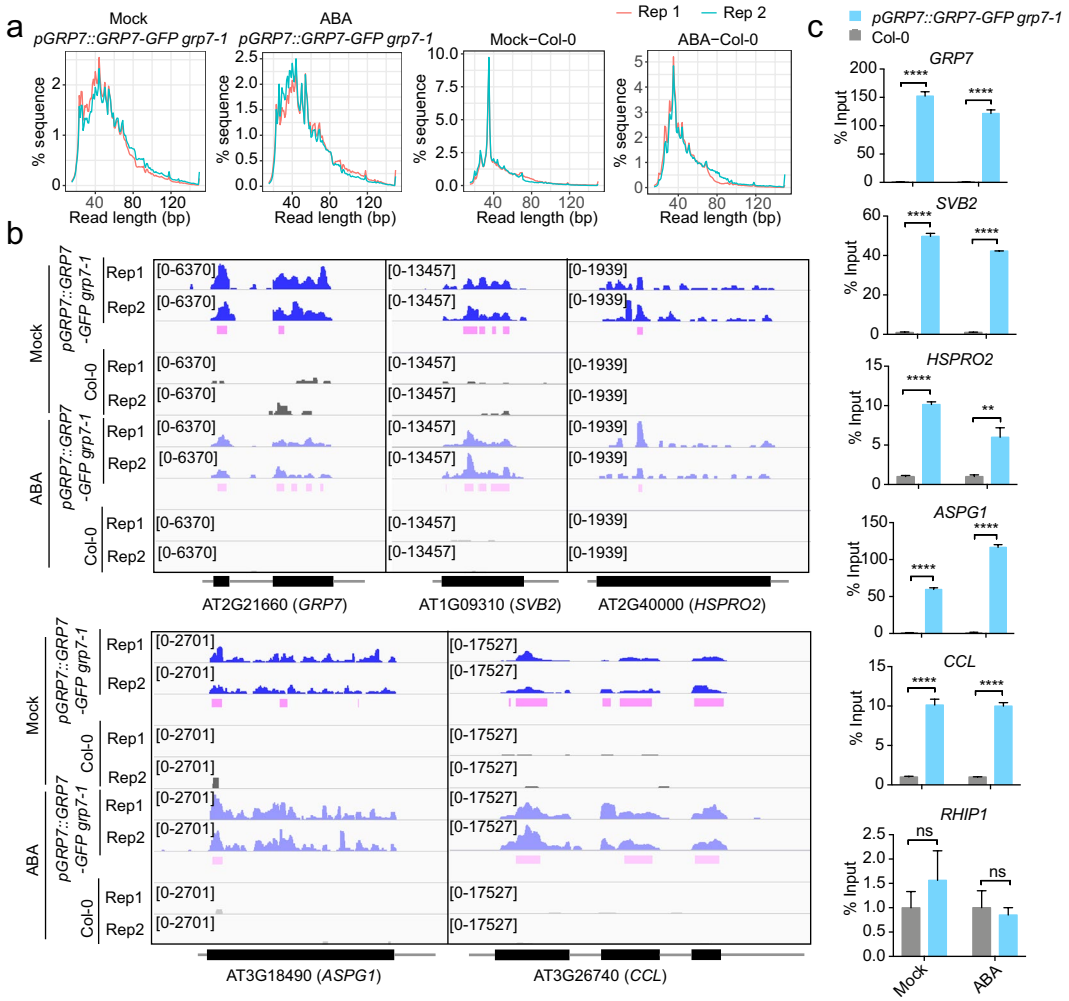

Fig. 5 Reads quality and technical validation of CLIP-seq of Col-0 and *pGRP7::GRP7-GFP grp7-1* with ABA or mock treatment. (**a**) Length distribution of clean reads from CLIP-seq. (**b**) IGV genome browser tracks show significant CLIP crosslink sites on GRP7 target transcripts. *GLYCINE-RICH RNA-BINDING PROTEIN 7* (*GRP7*), *SVB-LIKE* (*SVB2*), *ORTHOLOG OF SUGAR BEET HS1 PRO-1 2* (*HSPRO2*), *ASPARTIC PROTEASE IN GUARD CELL 1* (*ASPG1*) and *CCR-LIKE* (*CCL*). (**c**) RIP-qPCR analysis of CLIP targets that are showed in (**b**) in *pGRP7::GRP7-GFP grp7-1* and Col-0 under ABA or mock treatment. The levels in the GFP-trap precipitate are presented relative to the levels in the input. The values represent the means ± SD of three replicates. Student's *t* test: ns, no significant; **, $p < 0.01$; ****, $p < 0.0001$. *RHIP1* as unbound transcripts serve as negative control.

Assessment of CLIP-seq data. The mapping of clean reads to the TAIR10 reference genome yielding a mapping rate of 14.56% to 26.98% (Table 5). High pearson correlation coefficients of CPM values indicate strong reproducibility between replicates (Table 3). A previous study outlined the binding landscape of GRP7 using RIP-seq and iCLIP-seq methods to identify GRP7 target genes[22]. In our research, we employed CLIP-seq and identified a larger number of GRP7 target genes, with significant overlap with those identified in the previous study (Fig. 4c). The BAM files from the CLIP-seq data were converted to bigwig format using bamCoverage and visualized with the Integrative Genomics Viewer (IGV)[45], highlighting significant binding peaks in IP samples (*pGRP7::GRP7-GFP grp7-1*) compared to control samples (Col-0) (Fig. 5b). Notable genes such as *GRP7* (AT2G21660)[4], *SMALLER TRICHOMES WITH VARIABLE BRANCHES-LIKE* (*SVB2*, AT1G09310)[46], and *ASPARTIC PROTEASE IN GUARD CELL 1* (*ASPG1*, AT3G18490)[47], which are involved in ABA response, were identified, along with the circadian clock-regulated *CCR-LIKE* (*CCL*, AT3G26740)[48] and *ORTHOLOG OF SUGAR BEET HS1 PRO-1 2* (*HSPRO2*, AT2G40000)[49], linked to basal disease resistance (Fig. 5b). RIP-qPCR assays confirmed that GRP7 binds to the mRNAs of *GRP7*, *SVB2*, *ASPG1*, *CCL*, and *HSPRO2* under both ABA and mock treatments, while the negative control *RGS1-HXK1 INTERACTING PROTEIN 1* (*RHIP1*, AT4G26410)[50], which encodes a protein to have a 3-stranded helical structure that is required for some glucose-regulated gene expression, showed no enrichment (Fig. 5c). Western blot analysis reveals that the GRP7-GFP fusion protein exhibits a high level of immunoprecipitation efficiency (Fig. 2b). The overall reads quality, mapping rates, and binding efficiency underscore the high quality of our CLIP-seq libraries.

Code availability

Code used for all processing and analysis is available at Github (https://github.com/yx-xu/GRP7-mediate-translational-regulation).

Received: 11 June 2024; Accepted: 18 December 2024;
Published online: 28 December 2024

References

1. Chen, K. *et al*. Abscisic acid dynamics, signaling, and functions in plants. *J. Integr. Plant Biol* **62**, 25–54 (2020).
2. Ng, L. M., MELCHER, K., THE, B. T. & XU, H. E. Abscisic acid perception and signaling: structural mechanisms and applications. *Acta Pharmacologica Sinica* **35**, 567–584 (2014).
3. Guo, J. *et al*. Involvement of Arabidopsis RACK1 in Protein Translation and Its Regulation by Abscisic Acid. *Plant Physiol.* **155**, 370–383 (2011).
4. Zhang, J. *et al*. Unveiling the regulatory role of GRP7 in ABA signal-mediated mRNA translation efficiency regulation. Preprint at https://doi.org/10.1101/2024.01.12.575370 (2024).
5. Yuan, S., Zhou, G. & Xu, G. Translation machinery: the basis of translational control. *Journal of Genetics and Genomics* **51**, 367–378 (2024).
6. Rodnina, M. V. The ribosome in action: Tuning of translational efficiency and protein folding. *Protein Science* **25**, 1390–1406 (2016).
7. Liu, Y., Beyer, A. & Aebersold, R. On the Dependency of Cellular Protein Levels on mRNA Abundance. *Cell* **165**, 535–550 (2016).
8. Ingolia, N. T., Ghaemmaghami, S., Newman, J. R. S. & Weissman, J. S. Genome-Wide Analysis *in Vivo* of Translation with Nucleotide Resolution Using Ribosome Profiling. *Science* **324**, 218–223 (2009).
9. Ingolia, N. T., Brar, G. A., Rouskin, S., McGeachy, A. M. & Weissman, J. S. The ribosome profiling strategy for monitoring translation *in vivo* by deep sequencing of ribosome-protected mRNA fragments. *Nat Protoc* **7**, 1534–1550 (2012).
10. Brar, G. A. & Weissman, J. S. Ribosome profiling reveals the what, when, where and how of protein synthesis. *Nat Rev Mol Cell Biol* **16**, 651–664 (2015).
11. Liu, Q. *et al*. Ribo-uORF: a comprehensive data resource of upstream open reading frames (uORFs) based on ribosome profiling. *Nucleic Acids Research* **51**, D248–D261 (2023).
12. Burd, C. G. & Dreyfuss, G. Conserved Structures and Diversity of Functions of RNA-Binding Proteins. *Science* **265**, 615–621 (1994).
13. Ho, J. J. D. *et al*. A network of RNA-binding proteins controls translation efficiency to activate anaerobic metabolism. *Nat Commun* **11**, 2677 (2020).
14. Ma, L. *et al*. Roles of Plant Glycine-Rich RNA-Binding Proteins in Development and Stress Responses. *IJMS* **22**, 5849 (2021).
15. Kim, J. S. *et al*. Glycine-rich RNA-binding protein7 affects abiotic stress responses by regulating stomata opening and closing in *Arabidopsis thaliana*. *The Plant Journal* **55**, 455–466 (2008).
16. Kim, J. Y. *et al*. Glycine-rich RNA-binding proteins are functionally conserved in Arabidopsis thaliana and Oryza sativa during cold adaptation process. *Journal of Experimental Botany* **61**, 2317–2325 (2010).
17. Xiao, J. *et al*. AtJAC1 Regulates Nuclear Accumulation of GRP7, Influencing RNA Processing of FLC Antisense Transcripts and Flowering Time in Arabidopsis. *Plant Physiol.* **169**, 2102–2117 (2015).
18. Streitner, C. *et al*. An hnRNP-like RNA-binding protein affects alternative splicing by *in vivo* interaction with transcripts in Arabidopsis thaliana. *Nucleic Acids Research* **40**, 11240–11255 (2012).
19. Xu, F. *et al*. Phase separation of GRP7 facilitated by FERONIA-mediated phosphorylation inhibits mRNA translation to modulate plant temperature resilience. *Molecular Plant* **17**, 460–477 (2024).
20. Nicaise, V. *et al*. Pseudomonas HopU1 modulates plant immune receptor levels by blocking the interaction of their mRNAs with GRP7. *EMBO J* **32**, 701–712 (2013).
21. Schmal, C., Reimann, P. & Staiger, D. A Circadian Clock-Regulated Toggle Switch Explains AtGRP7 and AtGRP8 Oscillations in Arabidopsis thaliana. *PLoS Comput Biol* **9**, e1002986 (2013).
22. Meyer, K. *et al*. Adaptation of iCLIP to plants determines the binding landscape of the clock-regulated RNA-binding protein AtGRP7. *Genome Biol* **18**, 204 (2017).
23. Chen, S., Zhou, Y., Chen, Y. & Gu, J. fastp: an ultra-fast all-in-one FASTQ preprocessor. *Bioinformatics* **34**, i884–i890 (2018).
24. Dobin, A. *et al*. STAR: ultrafast universal RNA-seq aligner. *Bioinformatics* **29**, 15–21 (2013).
25. Liao, Y., Smyth, G. K. & Shi, W. featureCounts: an efficient general purpose program for assigning sequence reads to genomic features. *Bioinformatics* **30**, 923–930 (2014).
26. Love, M. I., Huber, W. & Anders, S. Moderated estimation of fold change and dispersion for RNA-seq data with DESeq. 2. *Genome Biol* **15**, 550 (2014).
27. Gu, Z., Eils, R. & Schlesner, M. Complex heatmaps reveal patterns and correlations in multidimensional genomic data. *Bioinformatics* **32**, 2847–2849 (2016).
28. Calviello, L. *et al*. Detecting actively translated open reading frames in ribosome profiling data. *Nat Methods* **13**, 165–170 (2016).
29. Tang, Y. *et al*. OsNSUN2-Mediated 5-Methylcytosine mRNA Modification Enhances Rice Adaptation to High Temperature. *Developmental Cell* **53**, 272–286.e7 (2020).
30. Cunningham, F. *et al*. Ensembl 2022. *Nucleic Acids Research* **50**, D988–D995 (2022).
31. Langmead, B. & Salzberg, S. L. Fast gapped-read alignment with Bowtie 2. *Nat Methods* **9**, 357–359 (2012).
32. Xiao, Z., Zou, Q., Liu, Y. & Yang, X. Genome-wide assessment of differential translations with ribosome profiling data. *Nat Commun* **7**, 11194 (2016).
33. Van Nostrand, E. L. *et al*. Robust transcriptome-wide discovery of RNA-binding protein binding sites with enhanced CLIP (eCLIP). *Nat Methods* **13**, 508–514 (2016).
34. Zhao, T. *et al*. Impact of poly(A)-tail G-content on Arabidopsis PAB binding and their role in enhancing translational efficiency. *Genome Biol* **20**, 189 (2019).
35. Lovci, M. T. *et al*. Rbfox proteins regulate alternative mRNA splicing through evolutionarily conserved RNA bridges. *Nat Struct Mol Biol* **20**, 1434–1442 (2013).
36. Quinlan, A. R. & Hall, I. M. BEDTools: a flexible suite of utilities for comparing genomic features. *Bioinformatics* **26**, 841–842 (2010).
37. Yu, G., Wang, L.-G., Han, Y. & He, Q.-Y. clusterProfiler: an R Package for Comparing Biological Themes Among Gene Clusters. *OMICS: A Journal of Integrative Biology* **16**, 284–287 (2012).
38. Tong, J. *et al*. ALBA proteins confer thermotolerance through stabilizing HSF messenger RNAs in cytoplasmic granules. *Nat. Plants* **8**, 778–791 (2022).
39. Chen, T. *et al*. The Genome Sequence Archive Family: Toward Explosive Data Growth and Diverse Data Types. *Genomics, Proteomics & Bioinformatics* **19**, 578–583 (2021).
40. CNCB-NGDC Members and Partners. *et al*. Database Resources of the National Genomics Data Center, China National Center for Bioinformation in 2022. *Nucleic Acids Research* **50**, D27–D38 (2022).
41. *National Genomics Data Center* https://ngdc.cncb.ac.cn/bioproject/browse/PRJCA020137 (2024).
42. *NCBI Sequence Read Archive* https://identifiers.org/ncbi/insdc.sra:SRP530528 (2024).

43. Xiang, Y. *et al*. Pervasive downstream RNA hairpins dynamically dictate start-codon selection. *Nature* **621**, 423–430 (2023).
44. Xu, G. *et al*. Global translational reprogramming is a fundamental layer of immune regulation in plants. *Nature* **545**, 487–490 (2017).
45. Robinson, J. T. *et al*. Integrative genomics viewer. *Nat Biotechnol* **29**, 24–26 (2011).
46. Hussain, S. *et al*. Involvement of ABA Responsive SVB Genes in the Regulation of Trichome Formation in Arabidopsis. *IJMS* **22**, 6790 (2021).
47. Yao, X., Xiong, W., Ye, T. & Wu, Y. Overexpression of the aspartic protease ASPG1 gene confers drought avoidance in *Arabidopsis*. *Journal of Experimental Botany* **63**, 2579–2593 (2012).
48. Lidder, P., Gutiérrez, R. A., Salomé, P. A., McClung, C. R. & Green, P. J. Circadian Control of Messenger RNA Stability. Association with a Sequence-Specific Messenger RNA Decay Pathway. *Plant Physiology* **138**, 2374–2385 (2005).
49. Murray, S. L., Ingle, R. A., Petersen, L. N. & Denby, K. J. Basal Resistance Against *Pseudomonas syringae* in *Arabidopsis* Involves WRKY53 and a Protein with Homology to a Nematode Resistance Protein. *MPMI* **20**, 1431–1438 (2007).
50. Huang, J.-P., Tunc-Ozdemir, M., Chang, Y. & Jones, A. M. Cooperative control between AtRGS1 and AtHXK1 in a WD40-repeat protein pathway in Arabidopsis thaliana. *Front. Plant Sci*. **6** (2015).

Acknowledgements

We thank Professor Wenfeng Qian (Institute of Genetics and Developmental Biology, the Chinese Academy of Science) for supporting Ribo-seq analysis. We thank Professors Dorothee Staiger (Bielefeld University, Germany) and Yiliang Ding (John Innes Centre, UK) for providing *pGRP7::GRP7-GFP grp7-1* complementary line. This work is supported by Beijing Natural Science Foundation Outstanding Youth Project (JQ23026), the National Key Research and Development Program of China (2021YFD1201500), and the Strategic Priority Research Program of the Chinese Academy of Sciences (XDA24010204).

Author contributions

J.X. conceived and supervised the study. J.Z. performed the experiments; Y.-X. X. performed bio-informatics analysis. J.X., J.Z. and Y.-X.X. wrote the manuscript.

Competing interests

The authors declare no competing interests.

Additional information

Correspondence and requests for materials should be addressed to J.X.

Reprints and permissions information is available at www.nature.com/reprints.

Publisher's note Springer Nature remains neutral with regard to jurisdictional claims in published maps and institutional affiliations.